

# A New Scalar Reynolds Stress Model For Non-Isothermal Wall Bounded Turbulent Flows

M.D. EL HAYEK

Mechanical Engineering Department

Notre Dame University, Zouk-Mosbeh, LEBANON

E-mail: [mhayek@ndu.edu.lb](mailto:mhayek@ndu.edu.lb)

*Abstract:* The present investigation concerns the development of advanced scalar turbulence modeling approaches and their application to the calculation of non-isothermal wall-bounded flow phenomena. A new scalar modeling technique based on scalar turbulent scales is proposed and implemented at a second-order modeling approach. Instead of the classical analogy concept between the mechanical and the scalar transport mechanisms, a scalar time scale, defined as the ratio of the temperature variance and its rate of dissipation or scalar dissipation rate, is used to tackle the scalar turbulence closure problem. A simple scalar Reynolds stress model, capable of predicting various heat transport problems, is developed and tested by comparing its results for a thermal boundary layer with its standard mechanical counterpart as well as first-order models like the  $k$ - $\epsilon$  model and the  $g$ - $\chi$  model, a scalar version of the standard  $k$ - $\epsilon$  model. Validation against experimental data is performed and shows clearly the benefits of adopting the right scales for the right phenomenon: mechanical scales for momentum transport and specific scalar scales for scalar transport.

*Key-Words:* Turbulence Scales, Turbulence Models, Thermal Boundary Layer, Turbulent Prandtl Number.

## 1 Introduction

The turbulent wall-bounded flows are largely encountered in engineering applications involving heat or mass transfer. The prediction of such problems requires the implementation of some robust numerical techniques to solve the partial differential equations governing the transport mechanisms. Furthermore, advanced turbulence closure techniques are needed to correctly model the combination of features specific of such flows: boundary layers, sublayers, etc.

Many turbulence models have been developed, ranging from the simplest or the mixing length model to the most advanced or the Reynolds stress model (RSM). Despite their wide use for general engineering applications, these models still show many discrepancies when applied to wall dominated flows. The causes are multiple: near-wall features, high Reynolds models, etc. All these causes are addressed in the literature by using artificial damping functions to force the models to become compatible with the vanishing turbulence intensity in the near-wall zone. A large number of the so-called low-Reynolds number models were developed and are used for specific applications, especially for convective heat transfer calculations. None of these models can be considered as universal. The problem is even worst when dealing with the scalar transport since for such phenomena,

additional difficulties have to be solved prior to using the resulting models. Among these is the largely used analogy concept, which appears at nearly all modeling levels: directly in the two-equation models through the use of the constant turbulent Prandtl number hypothesis and implicitly in the second order closures by using similar turbulence scales for momentum and heat transfer mechanisms. The strong anisotropy of the turbulent fluxes is another non-negligible feature characterizing the turbulent transport of heat and/or species and should be taken into account when developing specific models for the scalar transport problem.

The analogy problem has been addressed, at the level of the two-equation model, by many investigations [1-3]. The main idea is to represent each flow phenomenon by its own scales: the hydrodynamics by the standard mechanical time scale ( $k/\epsilon$ ) and the scalar transport by a specific scalar time scale instead of the same ratio  $k/\epsilon$ . Several choices may be considered for the scalar time scale but a natural choice seems to be the ratio of the variance of temperature over its scalar rate of dissipation ( $g/\chi$ ). Such a change from  $k/\epsilon$  to  $g/\chi$  in modeling the scalar transport mechanism proved to be highly beneficial. The use of scalar scales along with the classical mechanical ones is more and more encountered in the literature [3].

The anisotropy can be naturally accommodated by using an appropriate Reynolds stress closure. Of this latter kind, the present study adopts the standard model for its more universal nature [4]. The standard Reynolds stress model was then extended by using an appropriate scalar time scale to close the turbulent flux equations in a manner similar to that adopted for the two-equation model [3]. The ratio  $g/\chi$  is used to model the different terms that require modeling in the turbulent flux equations. The result is a new kind of simple engineering scalar Reynolds stress model (SRSM), which has to be compared with more sophisticated Reynolds stress models and their cumbersome algebraic treatment like the cubic model [5].

The wall boundary conditions are critical when dealing with wall-bounded flows numerically. In spite of their shortcomings, wall functions remain the best solution for flows of engineering interest. In this regard, the present investigation makes use of an extended wall function approach developed especially to accommodate the new scalar turbulence parameters.

The advantages and disadvantages of the new turbulence model are discussed in light of comparisons with experimental data. The results show clearly the benefits of the scalar modeling approach and its promising features when dealing with wall bounded flows. Similar improvements were obtained in previous investigations considering free flow phenomena [6].

## 2 Governing Equations

The most appropriate equations to describe flow fields are the classical Navier-Stokes equations. For turbulent flows, however, and as a result of the complex nature of such flows, the more practical Reynolds averaged Navier-Stokes (RANS) equations are most often considered

$$\frac{\partial \rho U_j}{\partial x_j} = 0 \quad (1)$$

$$\frac{\partial \rho U_j U_i}{\partial x_j} = \frac{\partial}{\partial x_j} \left[ \mu \frac{\partial U_i}{\partial x_j} - \overline{\rho u_i u_j} \right] - \frac{\partial P}{\partial x_i} \quad (2)$$

$$\frac{\partial \rho U_j T}{\partial x_j} = \frac{\partial}{\partial x_j} \left[ \frac{k}{c_p} \frac{\partial T}{\partial x_j} - \overline{\rho u_j t} \right] + S_\theta \quad (3)$$

The main problem with such transformed equations is the fact that they involve more unknowns than equations. Usually turbulence models in more or less elaborate forms are used to determine the statistical unknowns, namely, the Reynolds stresses  $\overline{u_i u_j}$  and the turbulent fluxes  $\overline{u_j t}$ .

## 3 Turbulence Modeling

Many turbulence models have been developed and are widely used, with more or less success, to predict different kinds of engineering turbulent flows. Most of these models address mainly the mechanical aspect of the problem, e.g., the closure of the momentum equation. The heat transport aspect is generally handled by invoking some analogy concepts between the transport of momentum and heat. Experiments show, however, that the analogy can be used only in few limited cases (Prandtl number very close to unity, simple boundary layer flows, etc.). A completely different approach is needed for the heat transport problem or the transport of any scalar quantity in general. The main idea behind such a new modeling technique is to make each phenomenon governed by its own scales. The hydrodynamic aspect will continue to be characterized by the same mechanical scales: the turbulent kinetic energy, its dissipation rate and their derivatives. The transport of heat or the mixing is to be characterized by a set of scalar scales. To this end, the variance of temperature  $g$  and its rate of dissipation,  $\chi$ , or scalar dissipation rate are used.

The second order modeling approach is based on the fact that all the statistical unknowns appearing in the RANS equations (1-3) are governed by their transport equations

$$\frac{\partial \rho U_k \overline{u_i u_j}}{\partial x_k} = D_{ij} + P_{ij} + \Phi_{ij} - \frac{2}{3} \rho \varepsilon \delta_{ij} \quad (4)$$

$$\frac{\partial \rho U_k \overline{u_i t}}{\partial x_k} = D_{i\theta} + P_{i\theta} + \Phi_{i\theta} \quad (5)$$

where  $P_{ij}$  and  $P_{i\theta}$  represent the generation by mean fields given by

$$P_{ij} = -\overline{\rho u_i u_k} \frac{\partial U_j}{\partial x_k} - \overline{\rho u_j u_k} \frac{\partial U_i}{\partial x_k} \quad (6)$$

$$P_{i\theta} = P_{i\theta 1} + P_{i\theta 2} = -\overline{\rho u_i u_j} \frac{\partial T}{\partial x_j} - \overline{\rho u_j t} \frac{\partial U_i}{\partial x_j} \quad (7)$$

$D_{ij}$  and  $D_{i\theta}$  are the diffusion terms generally modeled using the generalized gradient diffusion hypothesis

$$D_{ij} = \frac{\partial}{\partial x_k} \left( C_c \tau_c \overline{\rho u_k u_i} \frac{\partial \overline{u_i u_j}}{\partial x_i} \right) \quad (8)$$

$$D_{i\theta} = \frac{\partial}{\partial x_k} \left( C_\theta \tau_\theta \overline{\rho u_k u_i} \frac{\partial \overline{u_i t}}{\partial x_i} \right) \quad (9)$$

In the standard Reynolds stress model (RSM), the Reynolds analogy is taken for granted and  $\tau_\theta$  is set equal to  $\tau_c$  or  $k/\varepsilon$ . The present investigation (SRSM) considers each diffusion phenomena to be governed by its own scale and the scalar time scale is then given by  $\tau_\theta = g/\chi$  instead of  $k/\varepsilon$ .

The next two terms or the pressure-strain correlation,  $\Phi_{ij}$ , and the pressure-temperature gradient correlation,  $\Phi_{i\theta}$ , are the most important due to their role in distributing the turbulent energy between the different stresses and fluxes. The modeling of these terms was and still is the most debated aspect of the second order modeling approach. In the frame of the standard Reynolds stress model, they are modeled as the superposition of two effects: the slow part or turbulence-turbulence interaction and the rapid part or the mean strain-turbulence interaction.

$$\Phi_{ij} = \Phi_{ij}^{(1)} + \Phi_{ij}^{(2)} + \Phi_{ijw}^{(1)} + \Phi_{ijw}^{(2)} \quad (10)$$

where  $\Phi_{ij}^{(1)}$  and  $\Phi_{ij}^{(2)}$  are modeled using the "return to isotropy" and the "isotropization of production" models [4], respectively,

$$\Phi_{ij}^{(1)} = -C_1 \frac{1}{\tau_c} \left( \overline{\rho u_i u_j} - \frac{2}{3} \rho k \delta_{ij} \right) \quad (11)$$

$$\Phi_{ij}^{(2)} = -C_2 \left( P_{ij} - \frac{1}{3} P_{kk} \delta_{ij} \right) \quad (12)$$

and  $\Phi_{ijw}^{(1)}$  and  $\Phi_{ijw}^{(2)}$  are modeled using the standard wall reflection models

$$\Phi_{ijw}^{(1)} = C_{1w} \frac{\rho}{\tau_c} \left( \overline{u_k u_l n_k n_l} \delta_{ij} - \frac{3}{2} \overline{u_i u_k n_j n_k} - \frac{3}{2} \overline{u_j u_k n_i n_k} \right) F_\alpha(x_n) \quad (13)$$

$$\Phi_{ijw}^{(2)} = C_{2w} \left( \Phi_{kl}^{(2)} n_k n_l \delta_{ij} - \frac{3}{2} \Phi_{ik}^{(2)} n_j n_k - \frac{3}{2} \Phi_{jk}^{(2)} n_i n_k \right) F_\alpha(x_n) \quad (14)$$

$F_\alpha$  is a function of the normal distance to the wall,  $x_n$ , used to damp the contribution of the wall terms to the pressure-strain correlation in the core of the flow. In the present study, an enhanced form is proposed and used,

$$F_\alpha(x_n) = \text{MIN} \left( \frac{C_\mu^{-1/4}}{\kappa} \frac{(\overline{uv})^2}{k^{1/2} \epsilon x_n}, \frac{C_\mu^{3/4}}{\kappa} \frac{k^{3/2}}{\epsilon x_n} \right) \quad (15)$$

Significant improvements were obtained when using equation (15) in lieu of the classical form [3].

Similar treatment of the turbulent heat fluxes allows the pressure-temperature gradient correlation to be written as

$$\Phi_{i\theta} = \Phi_{i\theta}^{(1)} + \Phi_{i\theta}^{(2)} + \Phi_{i\theta w}^{(1)} + \Phi_{i\theta w}^{(2)} \quad (16)$$

where the different components,  $\Phi_{i\theta}^{(1)}$ ,  $\Phi_{i\theta}^{(2)}$ ,  $\Phi_{i\theta w}^{(1)}$ , and  $\Phi_{i\theta w}^{(2)}$  are modeled using the following relationships

$$\Phi_{i\theta}^{(1)} = -C_{1\theta} \frac{1}{\tau_\theta} \overline{\rho u_i t} \quad (17)$$

$$\Phi_{i\theta}^{(2)} = -C_{2\theta} P_{i\theta 2} \quad (18)$$

$$\Phi_{i\theta w}^{(1)} = -C_{1\theta w} \rho \frac{1}{\tau_\theta} \overline{u_k t n_i n_k} F_\alpha(x_n) \quad (19)$$

$$\Phi_{i\theta w}^{(2)} = C_{2\theta w} \Phi_{k\theta}^{(2)} n_i n_k F_\alpha(x_n) \quad (20)$$

The last term of equation (4) represents the dissipation mechanism as modeled using the hypothesis of isotropic small scales. The mechanical dissipation rate is determined using a transport-like equation

$$\frac{\partial \rho U_j \epsilon}{\partial x_j} = \frac{\partial}{\partial x_j} \left[ C_\epsilon \frac{k}{\epsilon} \overline{\rho u_j u_k} \frac{\partial \epsilon}{\partial x_k} \right] + \frac{\epsilon}{k} (C_{\epsilon 1} P_{kk} - C_{\epsilon 2} \rho \epsilon) \quad (21)$$

The application of the same hypothesis to the turbulent fluxes leads to a null dissipation term as shown in equation (5).

The set of constants used in the standard Reynolds stress model is given in tables 1a and 1b.

Table 1a. Mechanical constants of the standard RSM.

$C_c$	$C_1$	$C_2$	$C_{1w}$	$C_{2w}$	$C_\epsilon$	$C_{\epsilon 1}$	$C_{\epsilon 2}$
0.22	1.8	0.6	0.5	0.3	0.18	1.44	1.92

Table 1b. Scalar constants of the standard RSM.

$C_\theta$	$C_{1\theta}$	$C_{2\theta}$	$C_{1\theta w}$	$C_{2\theta w}$
0.2	3.0	0.5	0.5	0.0

The different constants involved in the SRSM model can be determined using simple flow cases for which experimental data are available. Here a simple identification procedure with the standard model constants, in conjunction with a constant time scale ratio hypothesis, is used to determine the scalar constants. Some numerical optimizations are then performed and the resulting set is given in table 2. Comparison of these values with their mechanical counterparts (table 1a) shows the good equivalence between the two sets. This means that the same constants may be used for different phenomena providing that the right scales are adopted.

Table 2. Scalar constants of the SRSM.

$C_\theta$	$C_{1\theta}$	$C_{2\theta}$	$C_{1\theta w}$	$C_{2\theta w}$
0.2	2.0	0.5	0.2	0.0

To complete the modeling procedure, additional means are needed to evaluate the scalar time scale components,  $g$  and  $\chi$ . Like their mechanical counterparts,  $g$  and  $\chi$  are evaluated using transport-like equations resulting from the energy conservation equation. After the necessary manipulations and modeling, these two equations become [3]

$$\frac{\partial \rho U_j g}{\partial x_j} = \frac{\partial}{\partial x_j} \left[ C_g \tau_\theta \overline{\rho u_j u_k} \frac{\partial g}{\partial x_k} \right] + P_g - \rho \chi \quad (22)$$

$$\frac{\partial \rho U_j \chi}{\partial x_j} = \frac{\partial}{\partial x_j} \left[ C_\chi \tau_\theta \overline{\rho u_j u_k} \frac{\partial \chi}{\partial x_k} \right] + \frac{\chi}{g} (C_{\chi 1} P_g - C_{\chi 2} \rho \chi) + \frac{\chi}{k} (C_{\chi 2} P_{kk} - C_{\chi 4} \rho \epsilon) \quad (23)$$

$P_g$  is the production terms of the temperature variance by the mean flow field,

$$P_g = -\rho u_j t \frac{\partial T}{\partial x_j} \quad (24)$$

Here too, the different constants can be determined using simple flow fields for which it is possible to simplify the governing equations and then solve them analytically. The resulting values are then further refined by numerical tuning to reach the set given in table 3.

Table 3. Constants for the g- $\chi$  equations.

$C_g$	$C_\chi$	$\sigma_g$	$\sigma_\chi$	$C_{\chi 1}$	$C_{\chi 2}$	$C_{\chi 3}$	$C_{\chi 4}$
0.2	0.2	1.0	1.0	1.0	0.44	1.12	0.82

It is worth mentioning that the scalar scales are usually incorporated automatically into advanced second order modeling approaches [5]. By doing so, an implicit recognition of the fact that the scalar fields should be governed in a way or another by their own scales is formulated. The present study develops such an idea to its fullest extent while trying to keep the models as simple as possible.

In wall-bounded flows, the assumption of high Reynolds numbers ceases to be valid in the near wall zones where the viscous forces become non-negligible. Special treatment is required to solve the near-wall behavior. The most universal approach is to modify the models in order to take into account the specific features of the near wall zone. Many models have been developed in this regard and unfortunately, none can be considered universal. Moreover, such models require generally very fine meshes near the walls, a requirement that is very expensive when considering flow and heat transfer problems of engineering interest.

Owing to that, a simpler approach is often recommended, especially when considering flows of engineering interest where the resolution of the near-wall zones becomes an obstacle [7]. It consists of advanced wall function techniques used to jump over the near-wall zone from the wall itself to the turbulent layer. In the present study, the classical two-layer wall function is used for the flow and a scalar version is developed and used to represent the behavior of the scalar transport in the near wall region [3].

## 4 Numerical Technique

The new turbulence model has been implemented into a research computational fluid dynamics code [3]. The well known finite volume method is used with different algorithms to handle the pressure-

velocity coupling and several differencing schemes to discretize the convective transport terms. In the present study, the SIMPLEC algorithm has been used along with a power law scheme. Staggered non-uniform grids are used to map the calculation domains.

## 5 Thermal Boundary Layer

The whole procedure is used to predict the hydrodynamics as well as the thermal behavior of a turbulent boundary layer flow developing along a flat plate subjected to a sudden change of surface heat flux, [8]. The geometry is a flat plate 3.9m long subjected to a heat flux of 270 W/m<sup>2</sup> over the last 2.4m of its length (thermal boundary layer starts at  $X_0=1.5$ m). Air at  $T_0=26^\circ\text{C}$  is blown over the plate at a velocity of 9.45 m/s. The non-uniform mesh used consists of 220x75 control volumes along the streamwise and transversal directions, respectively. Numerical tests were carried out to ensure that the mesh is fine enough to result in a mesh independent solution without violating the requirements of the wall boundary conditions.

One generally and widely used criterion to check the validity of numerical techniques is the overall heat transfer coefficient represented here by the Stanton number as sketched in figure 1. Here the results of the two second order models (RSM and SRSM) are compared with experimental results. The results obtained with the standard k- $\epsilon$  and a scalar version, the g- $\chi$  model, are also represented for information.

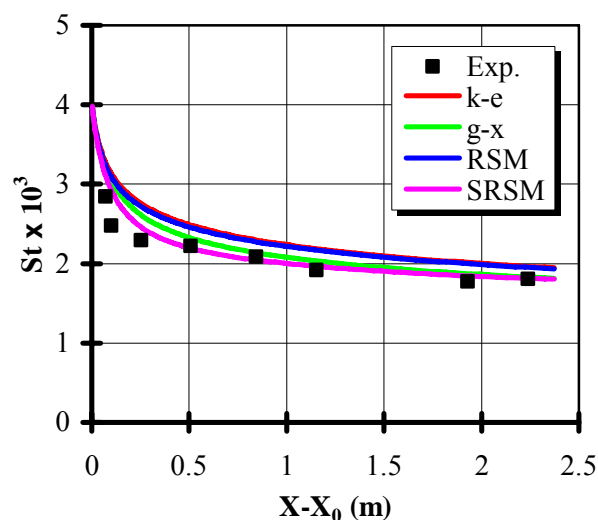


Fig.1. Stanton number along the plate.

The superior performance of the scalar models appears clearly although the mechanical models perform not bad. Such very good agreement is due mainly to the better predictions obtained with the

scalar models concerning the temperature distribution across the boundary layer as shown in figure 2 at two different locations along the streamwise direction ( $X^*$  being the streamwise distance from the entrance of the heated zone normalized by the boundary layer thickness at that entrance). Here the better representation of the thermal boundary layer development is shown since the scalar models perform much better at an earlier stage in the development process (figure 2a).

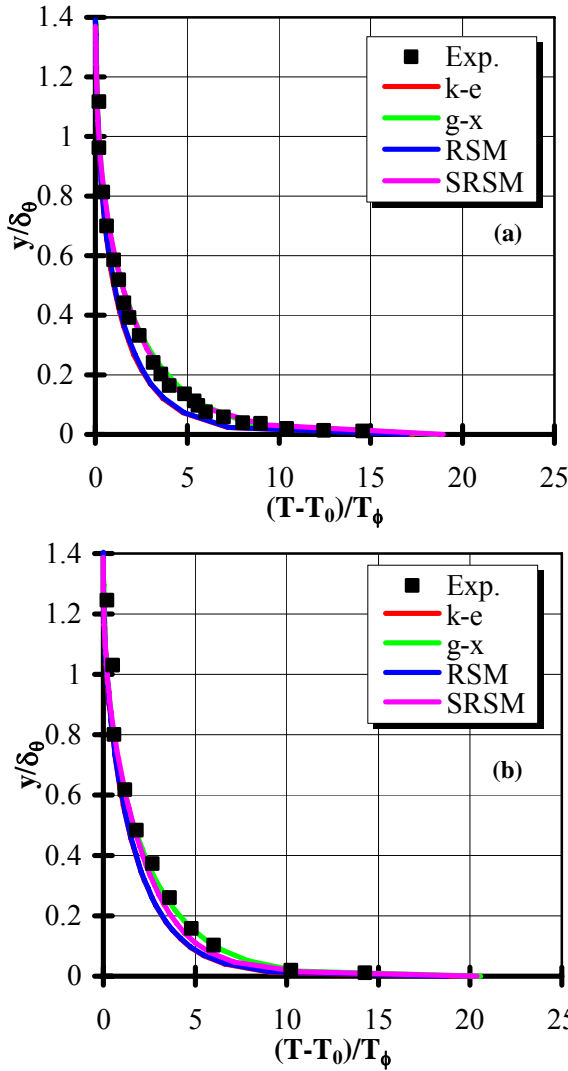


Fig.2 Mean temperature across the boundary layer, (a):  $X^*=18.9$ , and (b):  $X^*=42.9$ .

The transversal turbulent fluxes are shown in figure 3 where similar results are obtained by all the models of both first and second orders, mechanical and scalar forms. This is something usual since most models are tuned to predict correctly the behavior of the transversal turbulent heat flux across the boundary layer. The SRSM seems to predict a slightly higher values than the other models but the results remains within the error margins of the experimental data.

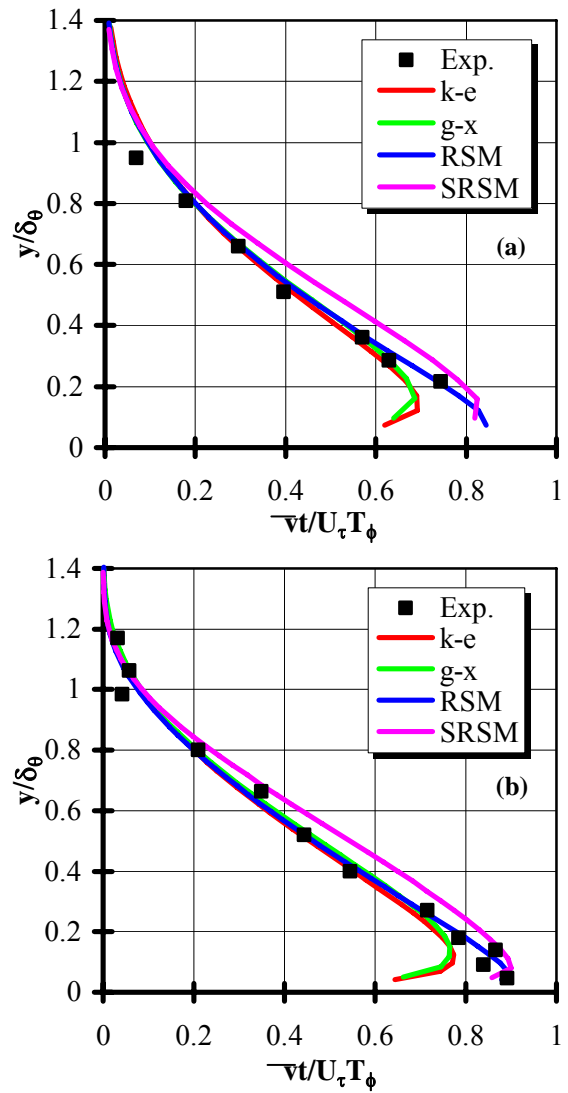


Fig.3 Transversal turbulent heat flux across the boundary layer, (a):  $X^*=18.9$ , and (b):  $X^*=42.9$ .

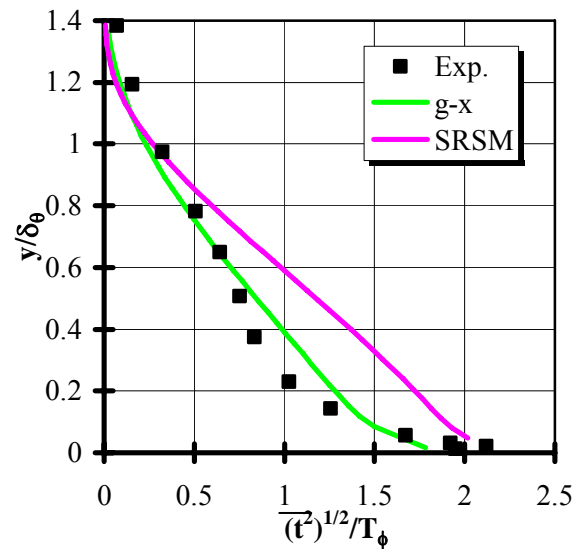


Fig.4 Temperature fluctuations across the boundary layer,  $X^*=42.9$ .

The predicted temperature fluctuations are compared in figure 4 with the corresponding experimental data. Here, obviously, the scalar models are shown only. The comparison between experiment and predictions is in favor of the  $g-\chi$  model. It means that the SRSM should be further tuned or improved in order to match correctly the experimental results.

Figure 5 shows the distribution of the turbulent Prandtl number across the boundary layer. It is clear that all the models fail to predict correctly  $Pr_t$ . The scalar models seem, however, much better than the mechanical ones in such a way that they predict a variable  $Pr_t$  and not a nearly constant as with the mechanical models. It is important to notice the ability of the scalar models to predict an increasing turbulent Prandtl number versus the distance to the wall in agreement with experimental data and analytical studies [9]. This is especially true far downstream where the two boundary layers, hydrodynamic and thermal, reach a steady development phase.

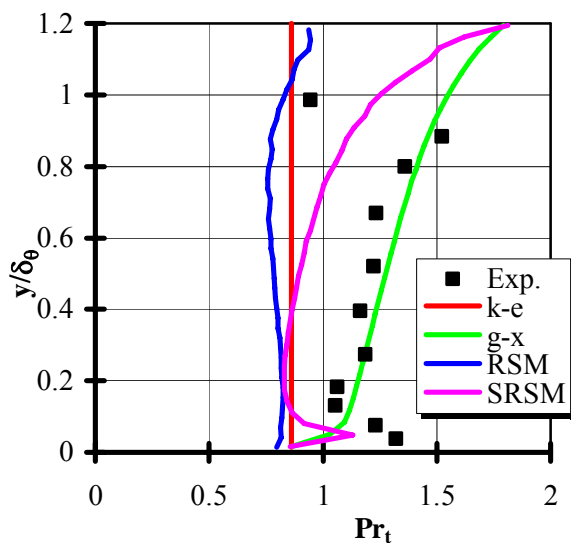


Fig.5 Turbulent Prandtl number across the boundary layer,  $X^*=42.9$ .

## 7 Conclusion

As a conclusion, the scalar modeling approaches achieve generally better prediction than their standard mechanical counterparts. Advanced modeling approaches involving very complicated mathematics are not always the panacea. Simpler scalar modeling approaches as presented here seem to be an attractive alternative owing to their simplicity. Of course, two supplementary equations have to be solved. This can be, however, achieved at very small cost since the extra CPU time required is

almost negligible. Furthermore, the scalar models deliver naturally additional quantities that may be needed in some applications in which the temperature fluctuations are critical design parameters.

## References:

- [1] Y. Nagano, C. Kim, A Two-Equation Model for Heat Transport in Wall Turbulent Shear Flows, *Transactions of the ASME - Journal of Heat Transfer*, Vol.110, 1988, pp.583-589.
- [2] M. El Hayek, J. Henriette, Turbulent Convective Heat Transfer Predictions with Two-Equation Scalar Turbulence Model, *ICHEME Symposium Series*, Vol.129, 1992, pp.955-961.
- [3] M. El Hayek, *Le transfert de chaleur par convection en régime turbulent: aspects physiques et numériques*, Thèse de Doctorat Européen, Faculté Polytechnique de Mons, Mons (Belgium), 1997.
- [4] B.E. Launder, G.J. Reece, W. Rodi, Progress in the Development of a Reynolds-Stress Turbulence Closure, *Journal of Fluid Mechanics*, Vol.68, 1975, pp.537-566.
- [5] T.J. Craft, *Second-Moment Modelling of Turbulent Scalar Transport*, Ph.D. Thesis, University of Manchester Institute of Science and Technology (UK), 1991.
- [6] M. El Hayek, Prediction of Heated Turbulent Jet Flow using Advanced Scalar Turbulence Models", paper IMECE2004-3002 in Proceedings of IMECE2004 "Recent Advances and Applications in Fluid Mechanics", Part I, Kuwait Society of Engineers, 2004, pp.15-32.
- [7] G. Kalitzin, G. Medic, G. Iaccarino, P. Durbin, Near-Wall Behavior of RANS Turbulence Models and Implementations for Wall Functions, *Journal of Computational Physics*, Vol.204, 2005, pp.265-291.
- [8] R.A. Antonia, H.Q. Danh, A. Prabhu, Response of Turbulent Boundary Layer to a Step Change in Surface Heat Flux, *Journal of Fluid Mechanics*, Vol.80, 1977, pp.153-177.
- [9] W.M. Kays, Turbulent Prandtl Number - Where Are We?, *Transactions of the ASME - Journal of Heat Transfer*, Vol.116, 1994, pp.284-295.